Atmos. Chem. Phys. Discuss., 11, 8207–8247, 2011
www.atmos-chem-phys-discuss.net/11/8207/2011/
doi:10.5194/acpd-11-8207-2011

Atmospheric Chemistry and Physics Discussions

A new method to detect long term trends of methane (CH_4) and nitrous oxide (N_2O) total columns measured within the NDACC ground-based high resolution solar FTIR network

J. Angelbratt[1], J. Mellqvist[1], T. Blumenstock[5], T. Borsdorff[4], S. Brohede[1], P. Duchatelet[2], F. Forster[4], F. Hase[5], E. Mahieu[2], D. Murtagh[1], K. Petersen[3], M. Schneider[5], R. Sussmann[4], and J. Urban[1]

[1]Chalmers University of Technology, Göteborg, Sweden
[2]Institute of Astrophysics and Geophysics, University of Liège, Liège, Belgium
[3]Institute of Environmental Physics, University of Bremen, Bremen, Germany
[4]Karlsruhe Institute of Technology (KIT), Institute for Meteorology and Climate Research (IMK-ASF), Garmisch-Partenkirchen, Germany

[5]Karlsruhe Institute of Technology (KIT), Institute for Meteorology and Climate Research (IMK-ASF), Karlsruhe, Germany

Received: 21 December 2010 – Accepted: 2 March 2011 – Published: 10 March 2011

Correspondence to: J. Mellqvist (johan.mellqvist@chalmers.se)

Published by Copernicus Publications on behalf of the European Geosciences Union.

ACPD
11, 8207–8247, 2011

Abstract

A multiple regression model has been used to estimate linear trends of the CH_4 and N_2O total columns measured with the ground-based solar FTIR technique at four European stations, i.e. Jungfraujoch (47° N, 8° E, 3600 m a.s.l.), Zugspitze (47° N, 11° E, 3000 m a.s.l.), Harestua (60° N, 11° E, 600 m a.s.l.) and Kiruna (68° N, 20° E, 400 m a.s.l.). The total columns were retrieved with a common method developed within the EU-project HYMN. Anomalies from air pressure, total columns of hydrogen fluoride (HF) and carbon monoxide (CO) and tropopause height were used in the regression model to reduce the time series variability and thereby estimate trustful trends. Significant positive CH_4 trends of 0.13–0.25% yr^{-1} at the 2-σ level were found for all participating stations for the 1996–2009 period. The strongest trends were estimated at northern latitudes stations while slightly weaker trends were observed in the Alps. For the time period of 2007–2009 a strong increase in the CH_4 total column was observed for all stations with the strongest yearly growth at Kiruna ($1.15 \pm 0.17\%\ yr^{-1}$). Significant positive N_2O trends of 0.19–0.40% yr^{-1} were found for all stations in the 1996–2007 period with the strongest trend at Harestua. From the N_2O data also crude tropospheric and stratospheric partial columns were derived, indicating that the observed difference in the N_2O trends between the FTIR sites is of stratospheric origin. This agrees well with the N_2O measurements by the Odin/SMR satellite showing the highest trends at Harestua $0.98 \pm 0.28\%\ yr^{-1}$, and considerably smaller trends in the alp regions $0.27 \pm 0.25\%\ yr^{-1}$. The multiple regression model was compared with two other trend methods, the ordinary linear regression and a Bootstrap algorithm. The multiple regression model estimated CH_4 and N_2O trends that differed by 12–31% compared to the other two methods. Since the trends estimated with the multiple regression model were carefully validated this stresses the importance to account for the atmospheric variability when estimating trends of CH_4 and N_2O total columns.

ACPD
11, 8207–8247, 2011

1 Introduction

Methane (CH_4) and nitrous oxide (N_2O) are among the largest contributors to the greenhouse effect (IPCC, 2007).

The CH_4 concentration in the atmosphere is to a large extent determined by the removal caused by the hydroxyl radical (OH) in the troposphere and the strength of the surface emissions (Dlugokencky et al., 1994). The emission sources are due to microbial activity primarily under anaerobic conditions in wetlands, rice paddies and landfills. Other important CH_4 emission sources are ruminants, natural gas leakage and fossil fuel and biomass burning. The amount of CH_4 in the atmosphere has increased during the later part of the twentieth century. Between 1978–1987 the growth rate was important, (i.e. 1,1% yr^{-1}), but during the late 1980 the growth rate was slowing down to 0.3–0.6% yr^{-1} and even lower growth rates were reported during the 1990s (Simpson et al., 2006). In the early 2000s the CH_4 growth rate was nearly zero. During 2007 and 2008 however, CH_4 was on the rise again and global growth rates of $0.47 \pm 0.04\%\ yr^{-1}$ and $0.25 \pm 0.04\%\ yr^{-1}$ were reported each respective year (Dlugokencky et al., 2009).

In contrast to CH_4, the dominant N_2O source, both natural and anthropogenic, is microbial activity under aerobic conditions in soils. The source is strongly linked with the use of synthetic nitrogen fertilizers, which have increased during the later part of the twentieth century (Davidson, 2009). Other important N_2O sources include: biomass burning, sewers, livestock and emission from transport and industries. The main sink for N_2O is photodissociation in the stratosphere by ultraviolet light and reaction with excited oxygen atoms (Prasad, 1997). Compared to the CH_4 trend, the N_2O accumulation in the atmosphere has been monotonic. During the last three decades, the atmospheric N_2O burden has shown an almost (constant) linear increase with a reported annual change of 0.26% yr^{-1} (IPCC, 2007).

This project was carried out within the EU project HYMN (Hydrogen, Methane and Nitrous Oxide, http://www.knmi.nl/samenw/hymn/) and one of the goals was to improve and homogenize the CH_4 and N_2O retrievals from high-resolution solar FTIR (Fourier

ACPD
11, 8207–8247, 2011

Transform Infra Red) measurements and to obtain, for both gases, total columns and vertical profiles as accurate as possible. Many of the participating ground-based FTIR stations have time series that cover 15 yr of data or more and it is therefore possible and interesting to study long term trends. Trends from greenhouse gases from FTIR measurements have earlier also been performed within the EU project UFTIR (http://www.nilu.no/uftir/) (Vigouroux et al., 2008).

One advantage when using FTIR total columns for the estimation of long term trends is their insensitivity to local variations of the atmosphere. In addition, since the global circulation is zonal in the free troposphere and stratosphere, the air stays at approximately the same latitude and the measurement station will therefore represent the atmosphere at that latitude. Hence, only a few stations at different latitudes are needed to represent the whole atmosphere. One disadvantage with FTIR is the fact that the time series often are uneven sampled since the solar absorption infrared measurements require clear sky conditions. Furthermore is there, for some stations, periods of missing data due to instrument failure and for the most northern stations because of the polar winter.

One of the common methods for estimating trends of atmospheric parameters is to use monthly average values (see for example Jones et al., 2009). The use of this method reduces the variability in the time series and removes the eventual periods of missing data. For an even sampled time series it is also possible to take the autocorrelation (also called serial correlation) into account (Tiao et al., 1990; Weatherhead et al., 1998). The FTIR data are autocorrelated on different timescales e.g., caused by meteorological patterns, seasonal cycles and other kinds of long-term variability. This correlation can best be described as a memory in the time series where a value at a certain time contains information of earlier values. Since our present FTIR time series include both uneven sampling and in some instance significant gaps it is difficult to create representative monthly averages. It is for some stations even impossible without interpolation. We use instead a multiple regression model, including a linear trend, a seasonal component and anomalies from various atmospheric parameters to account

ACPD
11, 8207–8247, 2011

for the time series variability to estimate trustful trends. The method also gives a possibility to quantify the atmospheric parameters that affect the measured time series through their contributions to the fitted regression model.

2 FTIR measurements and data retrieval

In this paper we use total column time series of CH_4, N_2O, carbon monoxide (CO), hydrogen fluoride (HF) and ethane (C_2H_6) measured with FTIR spectrometers at four European stations within the NDACC network (Network for the Detection of Atmospheric Composition Change, http://www.ndsc.ncep.noaa.gov/). FTIR measurements are performed since the mid 1990s, both in the Northern and Southern hemispheres. Information about the stations, instrumentations and retrievals are presented in Table 1. The CH_4 and N_2O trend analysis presented in our study covers the 1996–2009 or 1996–2007 time periods, for Jungfraujoch, Zugspitze, Harestua and Kiruna, respectively.

All the FTIR spectrometers involved in this study operate in the mid infrared spectral region from 700 cm^{-1} to 5000 cm^{-1} (2 to 14 µm) and measure the molecular absorption of solar light in the atmosphere for a wide range of species. Derived atmospheric abundance is expressed in terms of total column, defined as the sum of molecules from the top of the atmosphere down to the measurement station, per unit area (often expressed as molecules per square centimetre). To be able to spectrally resolve the atmospheric absorption lines for a given species, high resolution spectrometers are needed. For the stations in this paper a typical spectral resolution of 0.0035–0.005 cm^{-1} is used under operation.

During the retrieval process a synthetic spectrum, based on a priori information of pressure, temperature, trace gas profiles and instrumental characteristics, is calculated, by utilizing a forward model, dividing the atmosphere into 41–66 layers and calculate the light propagation through these. The calculated spectrum is then fitted to the FTIR measurements by varying the mixing ratio profile of the target species together with interfering species such as H_2O and CO_2. In this manner vertical profile of the target species can be obtained. These are generally calculated into total columns using

ACPD
11, 8207–8247, 2011

the available pressure and temperature information but for some species the data can also be divided into partial columns for instance dividing the total column into a tropospheric and stratospheric part. The height information available from the spectra is usually defined as the degrees of freedom (DOFs) which is obtained from averaging kernel calculations according the principles by Rodgers (2000).

The retrievals in this paper are performed by the two algorithms SFIT2 (Rinsland et al., 1998) and PROFFIT (Hase et al., 2004). The two codes have shown to be in excellent agreement with a deviation of only 1% or less (Hase et al., 2004). To quantify the instrument performance regarding line broadening and phase shift gas-cell measurements are done continuously on all instruments. These measurements are evaluated with the LINEFIT program (Hase et al., 1999).

The CH_4 and N_2O retrievals are done with a common strategy developed within the EU project HYMN, where the micro-windows, spectroscopic line lists, retrieval parameters, sources of ancillary data like pressure-temperature profiles, and water vapour data for deriving dry air columns are identical for all involved stations and used to minimize the errors between the stations. Except this a set of geophysical trace gas profiles are used on the FTIR stations.

In an earlier FTIR trend study by Gardiner et al. (2008), the retrievals was carried out by the optimal estimation algorithm (Rodgers, 2000). In this retrieval algorithm a cost function is minimized which corresponds to a weighted combination of a multiple least square solution and the apriori information. In the case of CH_4 and N_2O severe oscillations in the profiles are obtained and therefore instead a retrieval algorithm based on Tikhonov regularization (Twomey, 1996) has been applied to minimize this problem. In the latter retrieval algorithm, a cost function is minimized which corresponds to a weighted combination of a multiple least square solution and a cost term that corresponds to the first derivative of the vertical profile. The latter term minimize oscillations of the retrieved profile versus height but reduce the profile information to 2–3 independent partial columns (DOFs). For more information regarding FTIR retrieval with Tikhonov see Sussmann and Borsdorf (2007) and Sussmann et al. (2005).

ACPD
11, 8207–8247, 2011

In Table 2 detailed information regarding the HYMN retrieval parameters are presented. For both CH_4 and N_2O Hitran 2004 linelist parameters are used.

The CO, C_2H_6 and HF total columns, used as atmospheric parameters in the multiple regression model, are retrieved with standard procedures that have earlier been developed within the NDACC community (Mellqvist et al., 2002; DeMazière et al., 2005). The retrieval procedure varies slightly from site to site but use consistent micro window regions for CO (2057–2159 cm^{-1}), C_2H_6 (2976–2977 cm^{-1}) and HF (4038–4039 cm^{-1}).

3 The Odin satellite

The Sub-Millimetre Radiometer (SMR) onboard the Odin satellite, launched in Febuary 2001, observes thermal emission of a N_2O line at 502.3 GHz at the Earth limb. Measurements of the global N_2O field are obtained during about 15 (near polar, sun-synchronous) orbits per observation day and were performed time-shared with other operation modes on every third day until April 2007 and on every other day since then, providing a quasi-continuous N_2O data set from 2001 to 2010. N_2O in the stratosphere is retrieved between roughly 12–14 km and 60 km with a vertical resolution of about 1.5 km and a single-scan precision of 10–15% (below 30 km). For the here relevant level-2 data version 2.1. See e.g. Murtagh et al. (2002); Urban et al. (2005b, a); Urban (2006) and Strong et al. (2008) for a description of the Odin mission and information of the N_2O measurements, error analysis and validation studies.

4 Trend method

4.1 Linear regression

Regression analysis is a technique to study the connection between a dependent variable and one or several independent variables. In this paper we mean the dependency between the independent variable, time, and the dependent variable, the measured

ACPD
11, 8207–8247, 2011

total column time series. The simplest way to detect a trend is by fitting a straight line with the least squares method to the data, the slope of the line then represents the trend. The estimated trend itself is useless without an estimate of its error which could be represented with a confidence interval. When calculating a trend and its confidence interval three assumptions are usually made: (1) the residuals (measured-model) is assumed to be free from autocorrelation, (Eq. 1) the distribution of the residuals is assumed to be approximately normal distributed and (2) the residuals are assumed to have equal variance. Large deviations from these assumptions will result in errors in the estimated trends (Weatherhead et al., 1998; Tiao et al., 1990). Methods have been developed to account for autocorrelation when estimating trends but they all need data which have equidistant time steps between the measurements. However, due to local weather conditions and available sunlight hour's time series derived from FTIR observations are not sampled evenly and typically contain gaps. It is hence not possible to make representative weekly or monthly averages and thereby get time series with constant time space. To reduce the time series variability and estimate trustful trends a multiple regression model is used in this paper.

4.2 Atmospheric parameters

Several atmospheric parameters that are assumed to affect the measured total column of CH_4 and N_2O are discussed in this section. Data from the Harestua station have been used to test the effect of various atmospheric parameters on the measured total columns of CH_4 and N_2O. The parameters that have shown to have a significant effect on the measured total columns of CH_4 and N_2O at the Harestua station have then been applied to the FTIR data from the other participating stations.

Changes in the air pressure due to meteorological fluctuations will change the amount of molecules above the measurement station. A high pressure is expected to result in a high total column and vice versa. CH_4 and N_2O have their highest partial columns close to ground level, where they are intensively produced, and are therefore expected to be very sensitive to fluctuations in the air pressure. The tropopause height

ACPD
11, 8207–8247, 2011

is expected to affect the stratospheric column of CH_4 and N_2O but also to stretch and compress the tropospheric column. A low tropopause height is thought to make the tropospheric contribution to the total column smaller and a high larger. The tropopause height data used here are from the ECMWF (European Centre for Medium Range Weather Forecasts, http://www.ecmwf.int/) model that defines the tropopause altitude as the lowest level where the lapse rate is 2 °C km^{-1} or less and no height within 2 km above this point exceeds this value. To account for the presence of the polar vortex a range of PV (polar vorticity) values, at different altitudes (10–25 km), is used obtained from the ECMWF model. A high PV value is expected to correspond to the presence of vortex air above the measurements site and hence a low stratospheric column of CH_4 and N_2O.

The total column of the stratospheric species HF has been used in several other studies, among them Toon et al. (1997) and Mellqvist et al. (2002), as a proxy for stratospheric transport. This transport involves the downward motion of airmasses when the station is inside the polar vortex, the changes in tropopause height and the vertical and horizontal motion of air masses in the stratosphere. Hence, a large total column of HF is expected to result in a large stratospheric and a small tropospheric column of CH_4 and N_2O. The HF is closely related to the PV.

CH_4, N_2O, CO and C_2H_6 are all produced in fossil fuel and biomass burning. The total columns of CO and C_2H_6 are therefore used as a proxy for large scale biomass burning events as the ones present in Canada and Russia during the summers of 1998, 1999, 2002 and 2003 (Yurganov et al., 2004, 2005). The total columns of C_2H_6 will in addition be used as a proxy for natural gas leakage. This has, as to our knowledge, not been tested on CH_4 and N_2O FTIR total columns before.

Other physical parameters that have been investigated, but found to have insignificant impact on the column variability of the target species are; the number of sunspots, the North Atlantic Oscillations (NAO) and the Quasi Biennial Oscillations (QBO).

ACPD
11, 8207–8247, 2011

4.3 Trend model

To estimate trends in the CH_4 and N_2O total column time series a multiple regression model is used. In the model we try to explain as much as possible of the structures in the measured total column of CH_4 and N_2O with atmospheric parameters, a background trend and a seasonal component. The background trend is represented by one or several continuous linear trends according to the piecewise regression concept described by Neter et al. (1990). The seasonal component consists of a sine function with a phase which has a period of 12 months. The 12 month seasonal cycle is strongest at the high altitude stations due to the well mixed air i.e. the low influence of local sources. A more advanced representation of the seasonal cycle, a third order Fourier series, has also been tested in the model but didn't improve the model compared to the basic one. To explain the time series variability, i.e. short term deviations from the background trend and seasonal fluctuations, anomalies derived from some of the atmospheric parameters described in Sect. 4.2 are used. These anomalies correspond to the detrended and deseasonalized time series of the atmospheric parameters.

To find the anomalies that affect the CH_4 and N_2O total columns all derived anomalies are inserted into the multiple regression model, presented in Eq. (1), and tested with the stepwise regression method. This means that the combination of anomalies that gives the best adjusted R^2 value and are statistically significant are used in the final trend model and all the others being excluded, for adjusted R^2 information see Sect. 4.4. We define statistically significant as a parameter which confidence interval excludes zero.

The anomalies, background trend and seasonal component are inserted in the model in Eq. (1) and solved with the least squares method.

ACPD
11, 8207–8247, 2011

$$y = \beta_0 + \beta_1 \sin(2\pi t) + \beta_2 \cos(2\pi t) + \sum_{i=3}^{I} \beta_i a(t)_{i-2} + \beta_{I+1} t$$

$$+ \beta_{I+2}(t - \mathrm{cp1})A + \beta_{I+3}(t - \mathrm{cp2})B + \varepsilon$$

$$\text{where} \begin{cases} t > \mathrm{cp1}, A = 1 \\ t \leq \mathrm{cp1}, A = 0 \\ t > \mathrm{cp2}, B = 1 \\ t \leq \mathrm{cp2}, B = 0 \end{cases} \quad (1)$$

Where t is the time in fraction of years and cp1 and cp2 are change points when the trend is expected to change direction or magnitude. For CH_4 possible change points in 1999 and 2007 have been reported by Dlugokencky et al. (2003, 2009). In a first trend estimation no change points will be used for CH_4 and N_2O while in a second estimation the change points of Dlugokencky et al. (2003, 2009) will be used for CH_4.When no change points are used only the first trend term in Eq. (1) will be present in the model. In Eq. (1) y is the dependent variable (CH_4 or N_2O) and β corresponds to the regression coefficients. The $a(t)_i$ terms represent the anomalies from the atmospheric parameters and ε is the residual or unexplained part of the model. The term is assumed to be normal distributed with a constant variance around zero and free from auto correlation. In the regression model the anomalies, $a(t)_i$, t and y must all be of the same length. This means that for a certain day in the CH_4 or N_2O time series there must exist corresponding data for all of the calculated anomalies. To estimate confidence intervals for the trends a method for hypothesis testing described by Montgomery et al. (2008) is used.

4.4 Deriving anomalies

To obtain anomalies from the atmospheric parameters presented in Sect. 4.2, a model consisting of a seasonal function and a polynomial with varying order is fitted to each

ACPD
11, 8207–8247, 2011

of the atmospheric parameters, Eq. (2). The fitted model is then subtracted from the original atmospheric time series. To find the optimal polynomial fit for each atmospheric parameter the adjusted R^2 value is used (Montgomery et al., 2008). The value basically reflects the size of the model residual but adjusts the value to the number of terms in the regression model. If no adjustment is used the residual always decrease when increasing the number of terms in the regression model, this favours over fitting. An adjusted R^2 value close to one indicates a small residual and a good model fit while zero indicates the opposite

$$y = \beta_0 + \beta_1 \sin(2\pi t) + \beta_2 \cos(2\pi t) + \beta_3 t + \beta_4 t^2 + \beta_5 t^3 \quad (2)$$

In Eq. (2) y is the dependent variable i.e. the atmospheric parameters (air pressure, tropopause height and so on) and β are the estimated regression coefficients. The optimal polynomial for each atmospheric process is found by step wise increasing the polynomial order, fit the models with the linear regression method and calculated the adjusted R^2 value. When the adjusted R^2 value no longer increases with more than 1% the best fit is said to be found and the corresponding polynomial order is used to derive the anomaly. In Fig. 1 the Harestua total column time series of CO with fitted model is presented in the upper panel and the derived anomalies in the lower panel.

5 Results

5.1 Regression model anomalies

The anomalies shown to affect the measured total columns of CH_4 are: the air pressure, the total column of CO and HF. Parameters affecting N_2O are: the air pressure, the total column of HF and the tropopause height. The air pressure, tropopause height and CO anomalies are derived using Eq. (2) along with a linear trend. For HF a second order polynomial is used in Eq. (2) for Harestua, Jungfraujoch and Zugspitze while a linear trend is used for the fit of the Kiruna dataset.

ACPD
11, 8207–8247, 2011

The relative contribution of each regression parameter on the measured total columns of CH_4 and N_2O (in % of the total columns of CH_4 and N_2O) is presented in Fig. 2a and b respectively. Here the median contribution and the range are shown. The air pressure anomalies have, in median, the largest contribution on both the measured total column of CH_4 and N_2O with an average of 0.87% of the measured total columns and a 5% maximum at Jungfraujoch N_2O.

The atmospheric parameter with the second largest contribution is the HF anomaly. The HF anomaly contribution on the total column of CH_4 is substantially smaller than the air pressure while the contribution to N_2O is similar to the one from the air pressure. In the Jungfraujoch and Zugspitze N_2O total columns the HF anomalies have a greater maximum contribution than the air pressure. The opposite is found for CH_4. The anomalies from HF, based on an average for all stations, contribute to the total columns of N_2O with 0.63% but only with 0.38% for CH_4.

The median CO anomaly effect on CH_4 varies from 0.14%, for Zugspitze to 0.21% for Kiruna. The median tropopause height anomaly effect on the N_2O total columns varies with values from 0.1% for Kiruna to 0.2% for Harestua. The median unexplained part of the model is very similar for the two species, 0.41 % for CH_4 and 0.42 % for N_2O. The largest unexplained part, for both species, is found at Harestua and the smallest is found at Jungfraujoch. The linear trend median effect on CH_4 is 1.6% while the average effect on N_2O is 0.8%. The median values for the seasonal parameters are here 0.6% and 1.0% for the respectively species.

Noteworthy is that some of the tested atmospheric anomalies were excluded from the final regression model because they resulted in a model with a lower adjusted R^2 value than a combination of similar anomalies. One example is the anomalies from CO and C_2H_6, which both are statistically significant but CO was used because of its higher adjusted R^2 value. If both are included in the model there is always a risk to introduce multicolinearity, i.e. linear dependency between the parameters, in the model.

ACPD
11, 8207–8247, 2011

5.2 CH_4 trends

The estimated linear trends from the multiple regression model are presented in Table 3 and the fitted models to the CH_4 time series are presented in Fig. 3. For all participating stations significant trends at the 2-σ level are found for the period of 1996–2009. The trends vary with latitude and weaker trends are observed at Jungfraujoch and Zugspitze ($0.16 \pm 0.01\%\,yr^{-1}$ and $0.13 \pm 0.01\%\,yr^{-1}$) and stronger trends at Harestua and Kiruna ($0.25 \pm 0.02\%\,yr^{-1}$ and $0.21 \pm 0.01\%\,yr^{-1}$). The trends at the Alpine stations are as expected in close agreement to each other due to their close geographical location. Earlier Gardiner et al. (2008) have estimated linear trends for FTIR data and these trends are close to the estimated ones in this paper, i.e. $0.40 \pm 0.06\%\,yr^{-1}$ for Harestua and $0.17 \pm 0.03\%\,yr^{-1}$ for Jungfraujoch. The data in the earlier paper corresponds to the years 1995–2004 and they were retrieved with standard optimal estimation as explained earlier and the trend were derived with the Bootstrap method, see discussion below.

Dlugokencky (2009) reports an increased CH_4 growth in 2007 and 2008 based on global averages from flask samples. The same author has also reported a near zero trend between 1999 and 2007 and a positive trend before that. To investigate if these features also are present in the FTIR data we have applied piecewise regression (Neter et al., 1990) with three independent linear trends, choosing 1999 and 2007 as changing points in the trend model, Table 3. For all stations significant positive CH_4 growth rates are found for the 1996–1999 time period. The estimated values are between $0.38\%\,yr^{-1}$ and $0.61\%\,yr^{-1}$. This could be compared with the globally averaged surface trend value of $0.45\%\,yr^{-1}$ based on the time period of 1984–1999 reported by Dlugokencky et al. (2003). For each station involved, no significant trends have been deduced for CH_4 for the 1999–2007 time period, this is in agreement with global surface CH_4 data for the time period of 2000–2006 (Dlugokencky et al., 2009). From 2007 to 2009 we found increased growth rates for all participating stations ranging from 0.57–$1.15\%\,yr^{-1}$. The station with largest growth rate is Kiruna for which a positive value of

ACPD
11, 8207–8247, 2011

$1.15 \pm 0.17\%\,yr^{-1}$ is found. For comparison, Dlugokencky et al. (2009) report global averaged surface values of $0.47 \pm 0.03\%\,yr^{-1}$ for 2007 and $0.25 \pm 0.03\%\,yr^{-1}$ for 2008. The same authors also report a $0.78 \pm 0.07\%\,yr^{-1}$ growth value for the polar northern latitudes in 2007 and $0.46 \pm 0.09\%\,yr^{-1}$ for the low northern latitudes in 2008. The increased growth rates seen by Dlugokencky et al. (2009) for 2007 and 2008 is hence also observed at all FTIR stations.

5.3 N_2O trends

The fitted N_2O models are presented in Fig. 4 and the estimated trends are listed in Table 3. The N_2O trends vary from approximately $0.2 \pm 0.01\%\,yr^{-1}$ at Jungfraujoch and Zugspitze to 0.29 ± 0.02 and $0.4 \pm 0.02\%\,yr^{-1}$ at the two stations located further north. Earlier IPCC (2007) has reported a N_2O trend for the last decade of $0.26\%\,yr^{-1}$. This trend is verified by Haszpra et al. (2008) and Rinsland et al. (2009) who both report surface trends of $0.25 \pm 0.003\%\,yr^{-1}$. The estimated N_2O trends for Jungfraujoch and Zugspitze are a bit weaker than the earlier reported trends but in close agreement to each other. The trends for Kiruna and especially Harestua are stronger than the reported trends and are not in agreement with each other. This trend discrepancy is unexpected since N_2O is well mixed in the atmosphere due to its tropospheric lifetime of 114 yr (Davidson, 2009).

To exclude that instrumental errors are the cause for the deviating N_2O trends we have estimated total column trends also for CO_2 from Harestua and Kiruna. CO_2 was used because its atmospheric circulation time is similar to the lifetime N_2O and that both of the species are measured with the same type of detector (InSb detector). The CO_2 retrieval was conducted in the 2620–2630 cm^{-1} region with Hitran08 line parameters (Kohlhepp and Hase, personal communication, 2010). The estimated CO_2 trends for the two stations showed to be very similar, $0.50 \pm 0.06\%\,yr^{-1}$ for Harestua and $0.56 \pm 0.04\%\,yr^{-1}$ for Kiruna on a 2-σ basis and this corresponds well to the trend of roughly 0.51% presented by IPCC (2007) (the trend is based on an increase of

ACPD
11, 8207–8247, 2011

19 ppm from 1995 to 2005). From this test it is concluded that the FTIR instruments at Harstua and Kiruna behaved well during the studied period.

To further investigate the trend discrepancy between the FTIR stations trends we derived tropospheric- and stratospheric partial columns from the FTIR data at each station. The partial columns was derived with a weight function described by Gardiner et al. (2008) which use the average tropopause height and its standard deviation, here taken from the ECMWF model. The trends in the partial columns were estimated with a function consists of a linear trend and a seasonal cycle with a phase. All the estimated tropospheric trends were in the range of $0.19 \pm 0.01\%\,yr^{-1}$ to $0.28 \pm 0.03\%\,yr^{-1}$ while the stratospheric trends showed large inter station variability with strong positive trends at Harestua and Kiruna and weak positive trends at Jungfraujoch and Zugspitze, Table 4. Earlier, Gardiner et al. (2008) also showed this behaviour.

To verify the latitudinal differences in stratospheric N_2O trends detected by the solar FTIR measurements a comparison with N_2O limb measurements from the Odin satellite, see Sect. 3, was carried out. To get a rough estimation of the stratospheric N_2O columns at three locations (Jungfraujoch/Zugspitze, Harestua and Kiruna) SMR data were retrieved from altitudes covering 14–30 km within a radius of 500 km centred at each location. The satellite data quality in terms of measurement response and retrieval error were studied for all three locations and shown to be close to one and random scattered at approximately 10% respectively. The stratospheric N_2O trends from the SMR instrument data were calculated with the same trend model as the tropospheric and stratospheric partial columns. The outcome of the trend study is presented in Table 4 and in Fig. 5. The rough FTIR-satellite comparison indicates that the stratospheric N_2O trends can vary with latitude. This has to the authors knowledge not been reported before. The strongest positive trends for both FTIR and satellite data are estimated at Harestua. A slightly weaker trend is seen in Kiruna and a much weaker trend is estimated in the Alp region. It hence seems that the difference in total column trends between the Alp region and Harestua and Kiruna is caused by the differences in the stratospheric column trends and it appears that the highest trend is found at

ACPD
11, 8207–8247, 2011

the vortex edge, above Harestua as observed by FTIR and the SMR onboard Odin. We don't have an explanation for this behaviour but is likely related to the atmospheric circulation, since N_2O has a very long lifetime which would smooth out differences in sources and sinks.

5.4 Model stability

To obtain the confidence intervals, the residual from the model is assumed to be normally distributed with constant variance around a mean value of zero and to be free from autocorrelation. The residual distributions from the regression models for all FTIR stations are shown in the lower left panel in Fig. 6a and b (for CH_4) and in Fig. 7a and b (for N_2O). These distributions indicate that the assumption of normal distribution is justified. In the lower right panels in Fig. 6a and b and Fig. 7a and b the residuals are plotted as a function of the fitted model. To justify the constant variance assumption the residuals are expected to be randomly scattered around a constant level of zero. In our case we conclude that this assumption is justified for all the regression models. Also, to verify the assumption that no autocorrelation is present in the time series we look at the residual as a function of time, this can be seen in the upper panel in Fig. 6a and b and Fig. 7a and b. Shapes such as cycles might indicate autocorrelation and may make the confidence intervals for the estimated trends larger. Based on the residual analysis we conclude that no strong autocorrelation is presented in any of the regression models.

When working with multiple regression models, one always needs to consider multicolinearity. Multicolinearity is when one or several of the independent variables in the regression model contain similar information, i.e. are linearly dependent. The presence of multicolinearity may result in physically unrealistic values or signs and large confidence intervals of the estimated regression coefficients. To investigate the presence of multicolinearity in the regression model the concept of the variance inflation factor, VIF factor, is used (Neter et al., 1990). A VIF factor of 1 indicates totally independent variables and a factor larger than 10 indicates serious multicolinearity in the model

ACPD
11, 8207–8247, 2011

(Neter et al., 1990). In our case the calculated VIF factors are well below 10 for all FTIR stations and both of the species under investigation.

To verify that the 1% criteria, earlier defined in Sect. 4.4, in the calculations of the anomalies is appropriate a sensitivity analysis is performed on all the regression models. In the analysis the estimated linear trend and the adjusted R^2 value is studied as the anomaly of one of the atmospheric parameters is changed, i.e. the order of the fitted polynomial to the parameter is changed. The change of the linear trend in the total columns of CH_4 and N_2O is largest when increasing from polynomial order zero to a first order and to a second order polynomial for the total column of HF (0, 1, 2) while for the other parameters the change is largest from zero to first (0, 1). At higher order of polynomial only very small changes in the estimated trends are observed. It can also be seen that the adjusted R^2 value not increase for polynomials with higher order than two for HF and one for the other parameters. From the sensitivity analysis we conclude that the 1% criteria is appropriate for deriving the anomalies.

5.5 Method comparison

The results of the multiple regression model has been compared to two other trend methods. The first method, referred to as the Bootstrap algorithm (Efron and Tibshirani, 1993; Gardiner et al., 2008), is based on the least squares fitting of a linear trend and a seasonal component to the data. From the residuals a large number of dataset is randomly sampled (Bootstrapped), these datasets represent the random effects in the data. Each of these dataset is then added to the original fitted function and a set of trends are estimated. The center point of the estimated trends represents the final trend estimation and the width is the confidence intervals. The bootstrap algorithm is a non parametric method since it does not rely on the normal distribution and equal variance assumption. The second tested trend method is a simple least squares fit of a straight line and a seasonal component including a phase, when using this method the normal distribution assumption is made. Linear trends were estimated by the multiple regression model, the Bootstrap algorithm and by the simple least squares fit of a

ACPD
11, 8207–8247, 2011

straight line and a seasonal component, for the 1996–2009 and 1996–2007 period for CH_4 and N_2O total columns respectively. The outcome of the study is presented in Table 5 which shows the estimated trends with associated 95% confidence limits.

The three trend methods show all results that are in close agreement to each other. In general, the multiple regression method has slightly smaller confidence intervals than the other two methods. The trends obtained from the Bootstrap algorithm and the model with a linear trend and seasonal function are very similar for all the participating FTIR stations and both the CH_4 and N_2O time series. The reason for this is that all the CH_4 and N_2O time series are close to normal distributed. In this case the Bootstrap resampling stage is not necessary and can in fact introduce errors in the trend estimate since it can create physically unrealistic time series, especially for the stations at northern latitudes. One example is the high CH_4 and N_2O values related to the presence of the polar vortex, typically during winter and early spring, which with the Bootstrap algorithm can be located to the summer or autumn season. When fitting a trend to these time series the estimated trend values will have an impact on the final trend result and potentially make the confidence intervals wider.

The trends estimated from the multiple regression method differ in magnitude with 12% to 31% compared to the other two methods. This difference is most likely because the multiple regression model takes the atmospheric variability into account and hence reduces the unexplained part of the trend model. From the method comparison and model stability analysis we conclude that the multiple regression model gives the most reliable trends since it takes the atmospheric variability into account and fulfils the statistical assumptions presented in Sect. 5.4.

6 Discussion and conclusion

Long term CH_4 and N_2O trends from solar FTIR total columns have been estimated at four European stations. The estimated trends show latitudinal differences with stronger trends for both species at the northern sites and weaker trends at the Alpine stations.

ACPD
11, 8207–8247, 2011

When it comes to CH_4 this latitudinal difference is not surprising since the atmospheric concentration of the species are highly influenced of local sources. At high latitudes wetland contributes up to 25% of the CH_4 total emissions and these wetlands have shown to be sensitive to climate change (Jackowicz-Korczynski et al., 2010). In addition Russian natural gas is produced at the same latitudes as Harestua and Kiruna. This might be two possible reason for the stronger trends detected at the northern latitude sites (Harestua and Kiruna) compared to the two Alpine stations.

The latitudinal difference in the estimated N_2O trends is compared to CH_4 unexpected. Atmospheric N_2O has a lifetime that is more than 12 times longer than that of CH_4, 120 yr instead of 9, and is thereby well mixed in the troposphere and relatively insensitive to local sources. In the Odin SMR comparison we conclude that the strong FTIR total column trends at Harestua and Kiruna most probably arise from very strong stratospheric trends at these stations. One possible explanation could be the strengthening of the Brewer Dobson circulation as described by Li et al. (2010). This circulation transports air masses from the tropical tropopause into the stratosphere and towards the poles. If the circulation gets stronger with time more N_2O is transported towards Harestua and Kiruna with a stratospheric trend as result. The stations located further south are less influenced of this transport and hence a weaker stratospheric trend is detected. Another possible reason to the trend differences could be a trend in the tropopause height due to climate change or other changes in the atmospheric dynamics. Linear trends were therefore estimated from the tropopause data, the earlier used ECMWF data, for the FTIR stations. All the estimated trends were close to zero and insignificant. From this we conclude that a change in the tropopause altitude most likely not is responsible for the stratospheric N_2O trends. We conclude that more studies are needed regarding the latitudinal difference in stratospheric N_2O.

ACPD
11, 8207–8247, 2011

Acknowledgements. This paper is funded by the EU project HYMN. The author would like to thank Anders Strandberg and Glenn Persson for Harestua FTIR measurement and Marston Johnston for ECMWF data. P. Duchatelet and E. Mahieu have further been supported by the Belgian Federal Science Policy Office (BELSPO, Brussels). The International Foundation High Altitude Research Stations Jungfraujoch and Gornergrat (HFSJG, Bern) is also acknowledged. T. Blumenstock, F. Hase and M. Schneider would like to thank the Institute of Space Physics (IRF) Kiruna and in particular Uwe Raffalski (IRF) for supporting the measurements at Kiruna. Odin is a Swedish-led satellite project funded jointly by the Swedish National Space Board (SNSB), the Canadian Space Agency (CSA), the Centre National d'Etudes Spatiales (CNES) in France and the National Technology Agency of Finland (Tekes). The Odin mission is since 2007 supported through the 3rd party mission programme of the European Space Agency (ESA).

References

Davidson, E. A.: The contribution of manure and fertilizer nitrogen to atmospheric nitrous oxide since 1860, Nat. Geosci., 2, 659–662, doi:10.1038/Ngeo608, 2009.

DeMazière, M., Vigouroux, C., Gardiner, T., Coleman, M., Woods, P., Ellingsen, K., Gauss, M., Isaksen, I., Blumenstock, T., Hase, F., Kramer, I., Camy-peyret, C., Chelin, P., Mahieu, E., Demoulin, P., Duchatelet, P., Mellqvist, J., Strandberg, A., Velazco, V., Notholt, J., Sussmann, R., Stremme, W., and Rockmann, A.: The exploitation of ground-based Fourier transform infrared observations for the evaluation of tropospheric trends of greenhouse gases over Europe, J. Int. Environ. Sci., 2, 283–293, 2005.

Dlugokencky, E. J., Steele, L. P., Lang, P. M., and Masarie, K. A.: The Growth-Rate and Distribution of Atmospheric Methane, J. Geophys. Res.-Atmos., 99, 17021–17043, 1994.

Dlugokencky, E. J., Houweling, S., Bruhwiler, L., Masarie, K. A., Lang, P. M., Miller, J. B., and Tans, P. P.: Atmospheric methane levels off: Temporary pause or a new steady-state?, Geophys. Res. Lett., 30, 1992, doi:10.1029/2003gl018126, 2003.

Dlugokencky, E. J., Bruhwiler, L., White, J. W. C., Emmons, L. K., Novelli, P. C., Montzka, S. A., Masarie, K. A., Lang, P. M., Crotwell, A. M., Miller, J. B., and Gatti, L. V.: Observational constraints on recent increases in the atmospheric CH_4 burden, Geophys. Res. Lett., 36, L18803, doi:10.1029/2009gl039780, 2009.

ACPD

11, 8207–8247, 2011

Efron, B. and Tibshirani, R.: An introduction to the bootstrap, Monographs on statistics and applied probability, 57, Chapman & Hall, New York, 16, 436 pp., 1993.
Gardiner, T., Forbes, A., de Mazière, M., Vigouroux, C., Mahieu, E., Demoulin, P., Velazco, V., Notholt, J., Blumenstock, T., Hase, F., Kramer, I., Sussmann, R., Stremme, W., Mellqvist, J., Strandberg, A., Ellingsen, K., and Gauss, M.: Trend analysis of greenhouse gases over Europe measured by a network of ground-based remote FTIR instruments, Atmos. Chem. Phys., 8, 6719–6727, doi:10.5194/acp-8-6719-2008, 2008.
Hase, F., Blumenstock, T., and Paton-Walsh, C.: Analysis of the instrumental line shape of high-resolution Fourier transform IR spectrometers with gas cell measurements and new retrieval software, Appl. Optics, 38, 3417–3422, 1999.
Hase, F., Hannigan, J. W., Coffey, M. T., Goldman, A., Hopfner, M., Jones, N. B., Rinsland, C. P., and Wood, S. W.: Intercomparison of retrieval codes used for the analysis of high-resolution, ground-based FTIR measurements, J. Quant. Spectrosc. Ra., 87, 25–52, doi:10.1016/j.jqsrt.2003.12.008, 2004.
Haszpra, L., Barcza, Z., Hidy, D., Szilagyi, I., Dlugokencky, E., and Tans, R.: Trends and temporal variations of major greenhouse gases at a rural site in Central Europe, Atmos. Environ., 42, 8707–8716, doi:10.1016/j.atmosenv.2008.09.012, 2008.
IPCC: Contribution of Working Group I to the Fourth Assessment Report of the Intergovernmental Panel on Climate Change, 2007, Cambridge University Press, Cambridge, United Kingdom and New York, NY, USA, 2007.
Jackowicz-Korczynski, M., Christensen, T. R., Backstrand, K., Crill, P., Friborg, T., Mastepanov, M., and Strom, L.: Annual cycle of methane emission from a subarctic peatland, J. Geophys. Res.-Biogeo., 115, G02009, doi:10.1029/2008jg000913, 2010.
Jones, A., Urban, J., Murtagh, D. P., Eriksson, P., Brohede, S., Haley, C., Degenstein, D., Bourassa, A., von Savigny, C., Sonkaew, T., Rozanov, A., Bovensmann, H., and Burrows, J.: Evolution of stratospheric ozone and water vapour time series studied with satellite measurements, Atmos. Chem. Phys., 9, 6055–6075, doi:10.5194/acp-9-6055-2009, 2009.
Li, F., Newman, P. A., and Stolarski, R. S.: Relationships between the Brewer-Dobson circulation and the southern annular mode during austral summer in coupled chemistry-climate model simulations, J. Geophys. Res.-Atmos., 115, D15106, doi:10.1029/2009jd012876, 2010.
Mellqvist, J., Galle, B., Blumenstock, T., Hase, F., Yashcov, D., Notholt, J., Sen, B., Blavier, J.-F., Toon, G. C., and Chipperfield, M. P.: Ground-Based FTIR observations of chlorine activation

ACPD
11, 8207–8247, 2011

and ozone depletion inside the Arctic vortex during the winter of 1999/2000, J. Geophys. Res., 107, 8263, doi:10.1029/2001JD00108, 2002.
Montgomery, D. C., Jennings, C. L., and Kulahci, M.: Introduction to time series analysis and forecasting, Wiley series in probability and statistics, Wiley-Interscience, Hoboken, NJ, 11, 445 pp., 2008.
Murtagh, D., Frisk, U., Merino, F., Ridal, M., Jonsson, A., Stegman, J., Witt, G., Eriksson, P., Jimenez, C., Megie, G., de la Noe, J., Ricaud, P., Baron, P., Pardo, J. R., Hauchcorne, A., Llewellyn, E. J., Degenstein, D. A., Gattinger, R. L., Lloyd, N. D., Evans, W. F. J., McDade, I. C., Haley, C. S., Sioris, C., von Savigny, C., Solheim, B. H., McConnell, J. C., Strong, K., Richardson, E. H., Leppelmeier, G. W., Kyrola, E., Auvinen, H., and Oikarinen, L.: An overview of the Odin atmospheric mission, Can. J. Phys., 80, 309–319, doi:10.1139/P01-157, 2002.
Neter, J., Wasserman, W., and Kutner, M. H.: Applied linear statistical models : regression, analysis of variance, and experimental designs, 3rd Edn., Irwin, Homewood, IL, 16, 1181 pp., 1990.
Prasad, S. S.: Potential atmospheric sources and sinks of nitrous oxide, 2. Possibilities from excited O-2, "embryonic" O-3, and optically pumped excited O-3, J. Geophys. Res.-Atmos., 102, 21527–21536, 1997.
Rinsland, C. P., Jones, N. B., Connor, B. J., Logan, J. A., Pougatchev, N. S., Goldman, A., Murcray, F. J., Stephen, T. M., Pine, A. S., Zander, R., Mahieu, E., and Demoulin, P.: Northern and southern hemisphere ground-based infrared spectroscopic measurements of tropospheric carbon monoxide and ethane, J. Geophys. Res.-Atmos., 103, 28197–28217, 1998.
Rinsland, C. P., Chiou, L., Boone, C., Bernath, P., Mahieu, E., and Zander, R.: Trend of lower stratospheric methane (CH_4) from atmospheric chemistry experiment (ACE) and atmospheric trace molecule spectroscopy (ATMOS) measurements, J. Quant. Spectrosc. Ra., 110, 1066–1071, doi:10.1016/j.jqsrt.2009.03.024, 2009.
Rodgers, C. D.: Inverse Methods for Atmospheric Sounding, Series on Atmospheric, Oceanic and Planetary Physics, 2, 55–63, 2000.
Simpson, I. J., Rowland, F. S., Meinardi, S., and Blake, D. R.: Influence of biomass burning during recent fluctuations in the slow growth of global tropospheric methane, Geophys. Res. Lett., 33, L22808, doi:10.1029/2006gl027330, 2006.
Strong, K., Wolff, M. A., Kerzenmacher, T. E., Walker, K. A., Bernath, P. F., Blumenstock, T., Boone, C., Catoire, V., Coffey, M., De Mazière, M., Demoulin, P., Duchatelet, P., Dupuy, E.,

ACPD
11, 8207–8247, 2011

Hannigan, J., Höpfner, M., Glatthor, N., Griffith, D. W. T., Jin, J. J., Jones, N., Jucks, K., Kuellmann, H., Kuttippurath, J., Lambert, A., Mahieu, E., McConnell, J. C., Mellqvist, J., Mikuteit, S., Murtagh, D. P., Notholt, J., Piccolo, C., Raspollini, P., Ridolfi, M., Robert, C., Schneider, M., Schrems, O., Semeniuk, K., Senten, C., Stiller, G. P., Strandberg, A., Taylor, J., Téard, C., Toohey, M., Urban, J., Warneke, T., and Wood, S.: Validation of ACE-FTS N_2O measurements, Atmos. Chem. Phys., 8, 4759–4786, doi:10.5194/acp-8-4759-2008, 2008.

Sussmann, R. and Borsdorff, T.: Technical Note: Interference errors in infrared remote sounding of the atmosphere, Atmos. Chem. Phys., 7, 3537–3557, doi:10.5194/acp-7-3537-2007, 2007.

Sussmann, R., Stremme, W., Buchwitz, M., and de Beek, R.: Validation of ENVISAT/SCIAMACHY columnar methane by solar FTIR spectrometry at the Ground-Truthing Station Zugspitze, Atmos. Chem. Phys., 5, 2419–2429, doi:10.5194/acp-5-2419-2005, 2005.

Tiao, G. C., Reinsel, G. C., Xu, D. M., Pedrick, J. H., Zhu, X. D., Miller, A. J., Deluisi, J. J., Mateer, C. L., and Wuebbles, D. J.: Effects of Autocorrelation and Temporal Sampling Schemes on Estimates of Trend and Spatial Correlation, J. Geophys. Res.-Atmos., 95, 20507–20517, 1990.

Toon, G. C., Blavier, J.-F., Sen, B., Salawitch, R. J., Osterman, G. B., Notholt, J., Rex, M., McElroy, C. T., and Russell, J. M.: Ground-based observations of Arctic O_3 loss during spring and summer 1997, J. Geophys. Res., 104, 497–510, 1997.

Twomey, S.: Introduction to the mathematics of inversion in remote sensing and indirect measurements, Dover Publications, Mineola, NY, 10, 237 pp., 1996.

Urban, J., Lautie, N., Le Flochmoen, E., Jimenez, C., Eriksson, P., de La Noe, J., Dupuy, E., Ekstrom, M., El Amraoui, L., Frisk, U., Murtagh, D., Olberg, M., and Ricaud, P.: Odin/SMR limb observations of stratospheric trace gases: Level 2 processing of $C_/O$, N_2O, HNO_3, and O-3, J. Geophys. Res.-Atmos., 110, D14307, doi:10.1029/2004jd005741, 2005a.

Urban, J., Lautie, N., Le Flochmoen, E., Jimenez, C., Eriksson, P., de La Noe, J., Dupuy, E., El Amraoui, L., Frisk, U., Jegou, F., Murtagh, D., Olberg, M., Ricaud, P., Camy-Peyret, C., Dufour, G., Payan, S., Huret, N., Pirre, M., Robinson, A. D., Harris, N. R. P., Bremer, H., Kleinbohl, A., Kullmann, K., Kunzi, K., Kuttippurath, J., Ejiri, M. K., Nakajima, H., Sasano, Y., Sugita, W., Yokota, T., Piccolo, C., Raspollini, P., and Ridolfi, M.: Odin/SMR limb observations of stratospheric trace gases: Validation of N_2O, J. Geophys. Res.-Atmos., 110, D09301, doi:10.1029/2004jd005394, 2005b.

ACPD
11, 8207–8247, 2011

Urban, J., Murtagh, D., Lautié, N., Barret, B., Dupuy, E., de La Noë, J., Eriksson, P., Frisk, U., Jones, A., Le Flochmoën, E., Olberg, M., Piccolo, C., Ricaud, P., and Rösevall, J.: Odin/SMR Limb Observations of Trace Gases in the Polar Lower Stratosphere during 2004–2005, Proc. ESA First Atmospheric Science Conference, edited by: Lacoste, H., ESA-SP-628, 2006.

Weatherhead, E. C., Reinsel, G. C., Tiao, G. C., Meng, X. L., Choi, D. S., Cheang, W. K., Keller, T., DeLuisi, J., Wuebbles, D. J., Kerr, J. B., Miller, A. J., Oltmans, S. J., and Frederick, J. E.: Factors affecting the detection of trends: Statistical considerations and applications to environmental data, J. Geophys. Res.-Atmos., 103, 17149–17161, 1998.

Vigouroux, C., De Mazière, M., Demoulin, P., Servais, C., Hase, F., Blumenstock, T., Kramer, I., Schneider, M., Mellqvist, J., Strandberg, A., Velazco, V., Notholt, J., Sussmann, R., Stremme, W., Rockmann, A., Gardiner, T., Coleman, M., and Woods, P.: Evaluation of tropospheric and stratospheric ozone trends over Western Europe from ground-based FTIR network observations, Atmos. Chem. Phys., 8, 6865–6886, doi:10.5194/acp-8-6865-2008, 2008.

Yurganov, L. N., Blumenstock, T., Grechko, E. I., Hase, F., Hyer, E. J., Kasischke, E. S., Koike, M., Kondo, Y., Kramer, I., Leung, F. Y., Mahieu, E., Mellqvist, J., Notholt, J., Novelli, P. C., Rinsland, C. P., Scheel, H. E., Schulz, A., Strandberg, A., Sussmann, R., Tanimoto, H., Velazco, V., Zander, R., and Zhao, Y.: A quantitative assessment of the 1998 carbon monoxide emission anomaly in the Northern Hemisphere based on total column and surface concentration measurements, J. Geophys. Res.-Atmos., 109, D15305, diu:10.1029/2004jd004559, 2004.

Yurganov, L. N., Duchatelet, P., Dzhola, A. V., Edwards, D. P., Hase, F., Kramer, I., Mahieu, E., Mellqvist, J., Notholt, J., Novelli, P. C., Rockmann, A., Scheel, H. E., Schneider, M., Schulz, A., Strandberg, A., Sussmann, R., Tanimoto, H., Velazco, V., Drummond, J. R., and Gille, J. C.: Increased Northern Hemispheric carbon monoxide burden in the troposphere in 2002 and 2003 detected from the ground and from space, Atmos. Chem. Phys., 5, 563–573, doi:10.5194/acp-5-563-2005, 2005.

ACPD
11, 8207–8247, 2011

Table 1. FTIR stations and measurement series included in the trend study.

	Jungfraujoch	Zugspitze	Harestua	Kiruna
Latitude (° N)	47	47	60	68
Longitude (° E)	8	11	11	20
Altitude (m a.s.l)	3600	3000	600	400
Instrument type	Bruker 120HR	Bruker 125HR[1]	Bruker 125M[2]	Bruker 125HR[3]
Retrieval code	SFIT2	SFIT2	SFIT2	PROFFIT
Number of measurement days (CH_4)	1135	818	599	642
Number of measurement days (N_2O)	1160	739	592	765
Time period (CH_4)	1996–2009	1996–2009	1996–2009	1996–2009
Time Time period (N_2O)	1996–2007	1996–2007	1996–2007	1996–2007

[1] before 2006 Zugspitze operated a Bruker 120HR,
[2] before 2008 Harestua operated a Bruker 120M and
[3] before 2007 Kiruna operated a Bruker 120HR.

ACPD
11, 8207–8247, 2011

Table 2. Microwindows with interfering species used to retrieve the CH_4 and N_2O total column time series.

Species	Microwindows (cm^{-1})	Interfering species
CH_4	2613.70–2615.40	HDO, CO_2
	2650.60–2651.30	HDO, CO_2
	2835.50–2835.80	HDO
	2903.60–2904.03	NO_2
	2921.00–2921.60	H_2O, HDO, NO_2
N_2O	2481.28–2482.62	CO_2, CH_4
	2526.40–2528.20	CO_2, CH_4, HDO
	2537.84–2538.82	CH_4
	2540.00–2540.75	CH_4

ACPD
11, 8207–8247, 2011

Table 3. Estimated linear trends from the multiple regression model. The trends are given as total column and as percent relative the average value of year 2000. The confidence intervals for each trend are based on a 95% significance level.

	Time period		Jungfraujoch (47° N, 8° E)	Zugspitze (47° N, 11° E)	Harestua (60° N, 11° E)	Kiruna (68° N, 20° E)
CH_4	1996–2009	mol cm^{-2} 10^{16}	3.85 ± 0.13	3.24 ± 0.29	8.63 ± 0.52	7.5 ± 0.38
		% yr^{-1}	0.16 ± 0.01	0.13 ± 0.01	0.25 ± 0.02	0.21 ± 0.01
	1996–1999	mol cm^{-2} 10^{16}	9.00 ± 0.92	14.60 ± 0.95	20.80 ± 3.53	16.10 ± 2.65
		% yr^{-1}	0.38 ± 0.04	0.57 ± 0.04	0.61 ± 0.10	0.46 ± 0.08
	1999–2007	mol cm^{-2} 10^{16}	1.57 ± 1.97	0.95 ± 1.96	7.39 ± 7.54	4.45 ± 5.68
		% yr^{-1}	0.07 ± 0.08	0.04 ± 0.08	0.22 ± 0.22	0.13 ± 0.16
	2007–2009	mol cm^{-2} 10^{16}	21.10 ± 1.79	24.50 ± 1.34	19.70 ± 7.54	40.30 ± 5.92
		% yr^{-1}	0.90 ± 0.08	0.96 ± 0.05	0.57 ± 0.22	1.15 ± 0.17
N_2O	1996–2007	mol cm^{-2} 10^{15}	8.6 ± 0.26	8.5 ± 0.56	23.6 ± 1.25	17.2 ± 1.40
		% yr^{-1}	0.21 ± 0.01	0.19 ± 0.01	0.40 ± 0.02	0.29 ± 0.02

ACPD
11, 8207–8247, 2011

Table 4. Stratospheric N_2O trends from SMR and FTIR data presented in % yr^{-1}. The trends are presented with associated 95% confidence intervals and use the 2005 average partial column as reference.

	Jungfraujoch	Zugspitze	Harestua	Kiruna
Odin/SMR (2001–2007)	0.27 ± 0.25		0.98 ± 0.28	0.60 ± 0.26
FTIR stratosphere (1996–2007)	0.15 ± 0.05	0.28 ± 0.07	1.13 ± 0.15	0.67 ± 0.12
FTIR troposphere (1996–2007)	0.27 ± 0.01	0.19 ± 0.01	0.28 ± 0.03	0.24 ± 0.03

ACPD
11, 8207–8247, 2011

Table 5. Estimated linear trends from the total columns of CH_4 and N_2O. The trends are presented in percent per year (% yr^{-1}) with the reference year given as the average value of year 2000. All trends are given with associated 95% confidence intervals.

Trend model	Species	Jungfraujoch	Zugspitze	Harestua	Kiruna
Multiple regression model	CH_4	0.16 ± 0.01	0.13 ± 0.01	0.25 ± 0.02	0.21 ± 0.01
	N_2O	0.21 ± 0.01	0.19 ± 0.01	0.40 ± 0.02	0.29 ± 0.02
Bootstrap algorithm	CH_4	0.16 ± 0.02	0.09 ± 0.03	0.28 ± 0.04	0.26 ± 0.04
	N_2O	0.25 ± 0.03	0.22 ± 0.03	0.45 ± 0.06	0.33 ± 0.05
Linear trend with seasonal component	CH_4	0.16 ± 0.01	0.09 ± 0.02	0.28 ± 0.03	0.26 ± 0.02
	N_2O	0.25 ± 0.02	0.22 ± 0.02	0.46 ± 0.04	0.34 ± 0.03

ACPD
11, 8207–8247, 2011

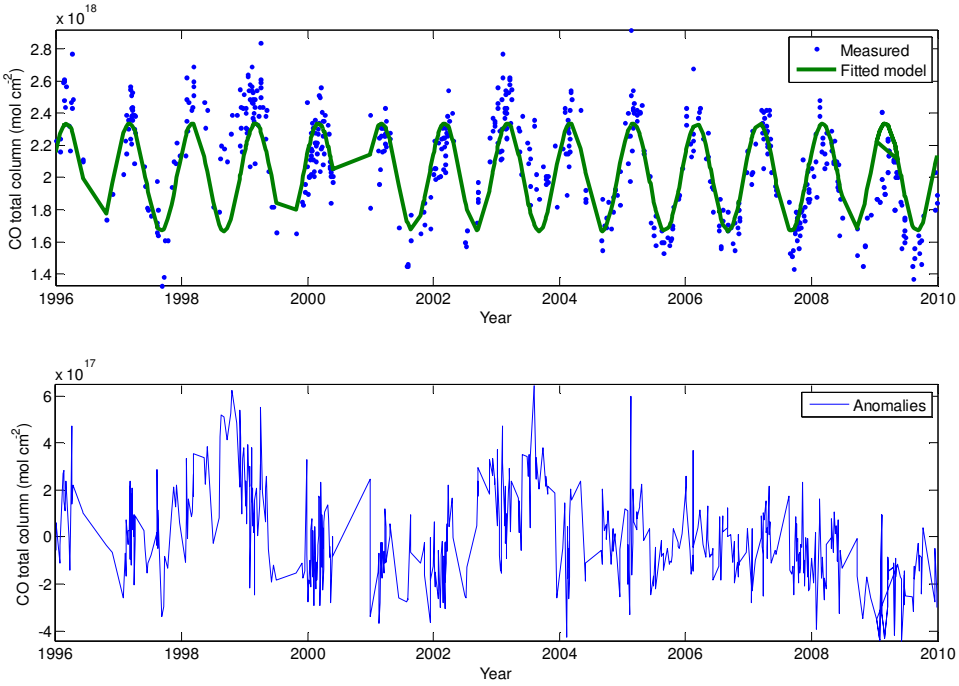

Fig. 1. Measured total column of CO at Harestua with fitted model (upper panel) and calculated anomalies (lower panel). To obtain the anomalies the fitted model is subtracted from the measured time series.

ACPD
11, 8207–8247, 2011

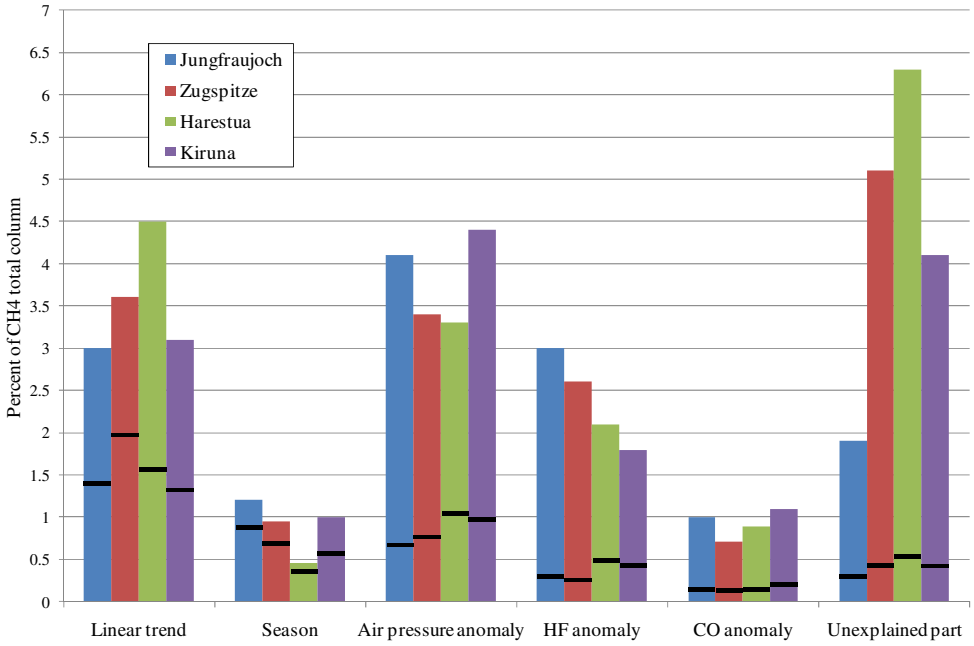

Fig. 2a. Relative contributions from each regression parameter (in %) on the measured total column of CH_4. The black lines indicate the median value for each parameter and the bar the minimum and maximum values.

ACPD
11, 8207–8247, 2011

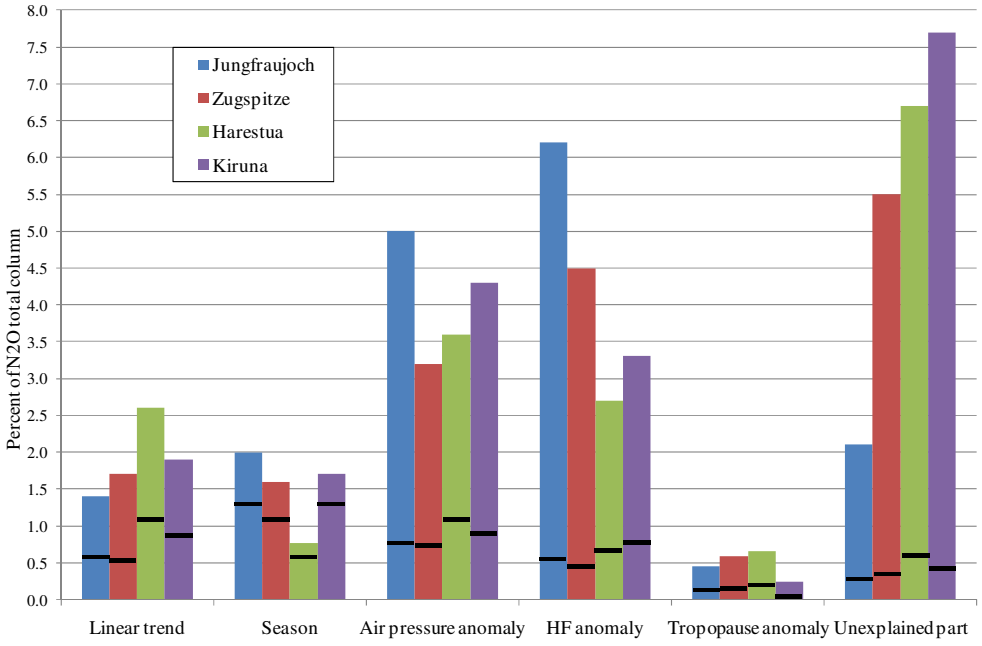

Fig. 2b. As Fig. 2a but for N_2O.

ACPD
11, 8207–8247, 2011

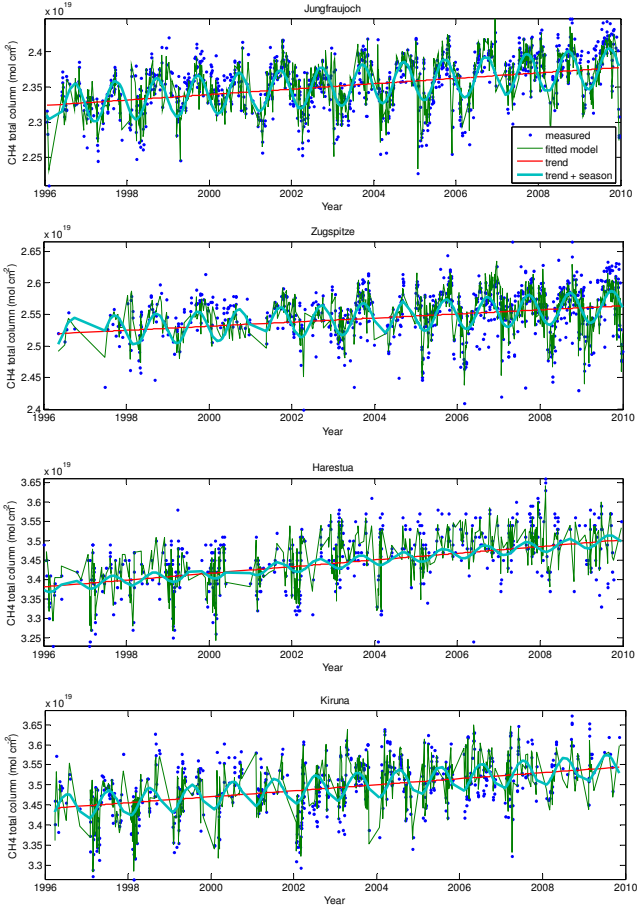

Fig. 3. CH_4 total column time series for all participating FTIR stations with fitted model, linear trend and seasonal cycle. The model is displayed in green and the measurements in blue, the seasonal cycle is displayed in thick cyan and the linear trend in red.

ACPD
11, 8207–8247, 2011

A new method to detect long term trends of CH_4 and N_2O

J. Angelbratt et al.

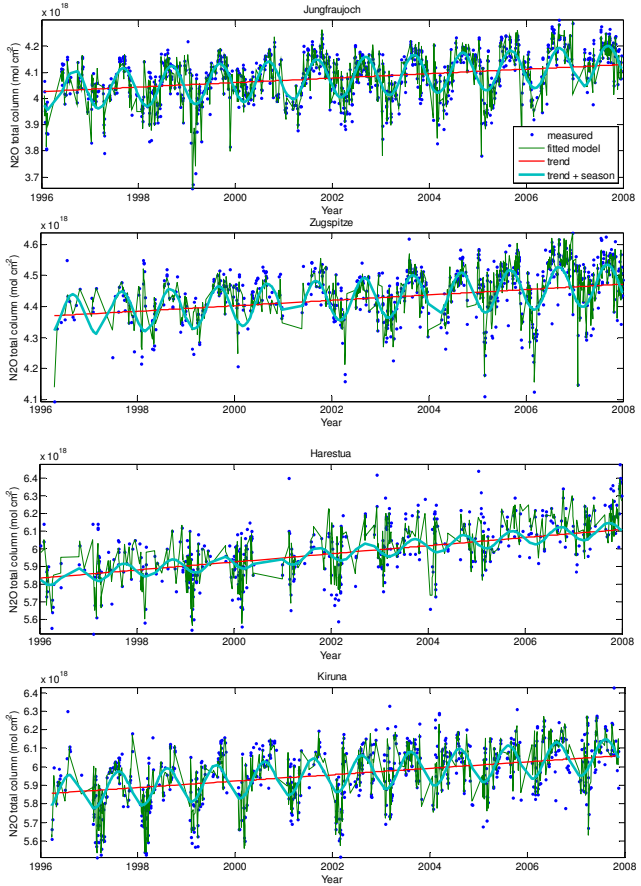

Fig. 4. As Fig. 3 but for N_2O total columns.

ACPD
11, 8207–8247, 2011

A new method to detect long term trends of CH_4 and N_2O

J. Angelbratt et al.

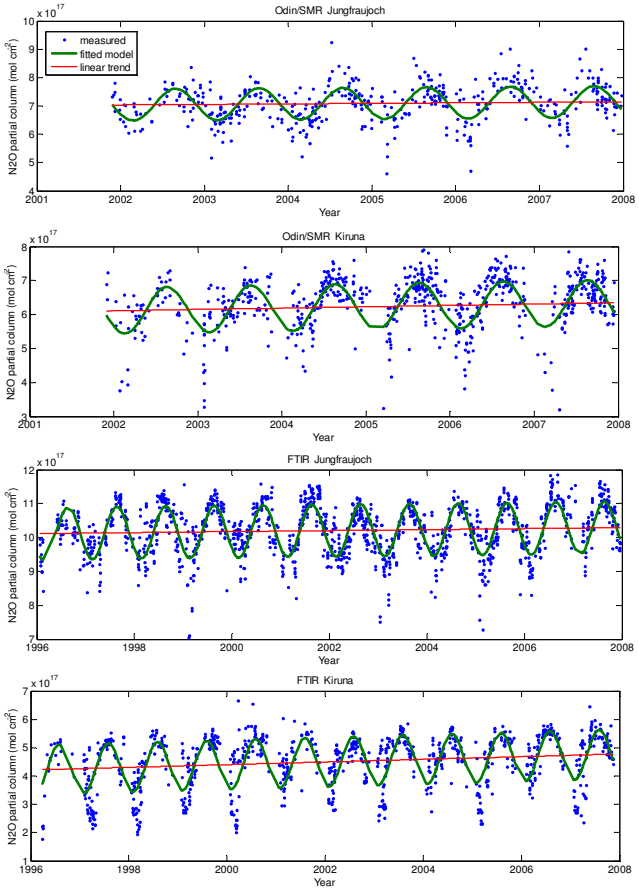

Fig. 5. Stratospheric partial columns of N_2O with fitted seasonal function and linear trend for Jungfraujoch and Kiruna from the Odin SMR satellite and solar FTIR data.

ACPD
11, 8207–8247, 2011

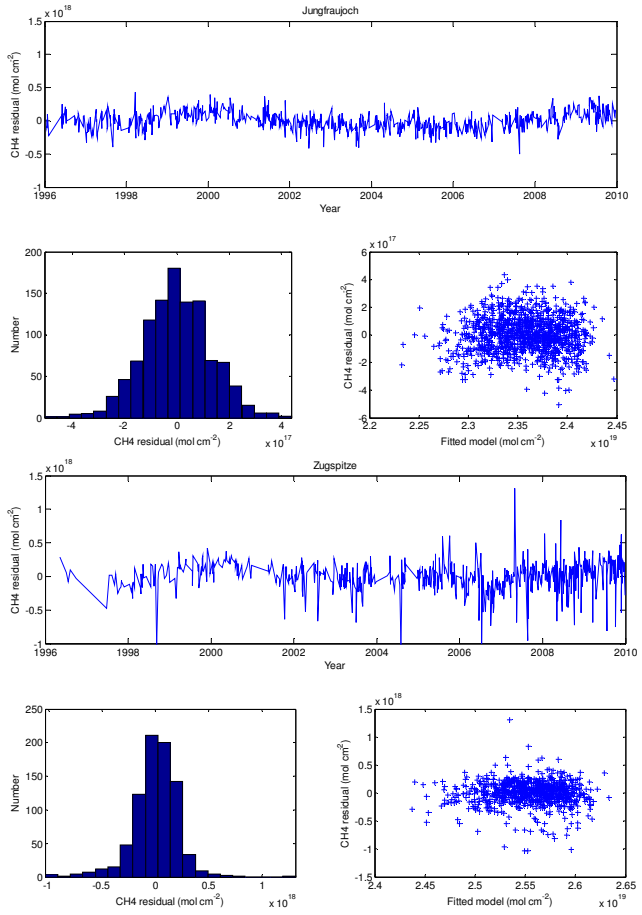

Fig. 6a. CH_4 residuals and distributions of the Jungfraujoch and Zugspitze FTIR time series.

ACPD
11, 8207–8247, 2011

A new method to detect long term trends of CH_4 and N_2O

J. Angelbratt et al.

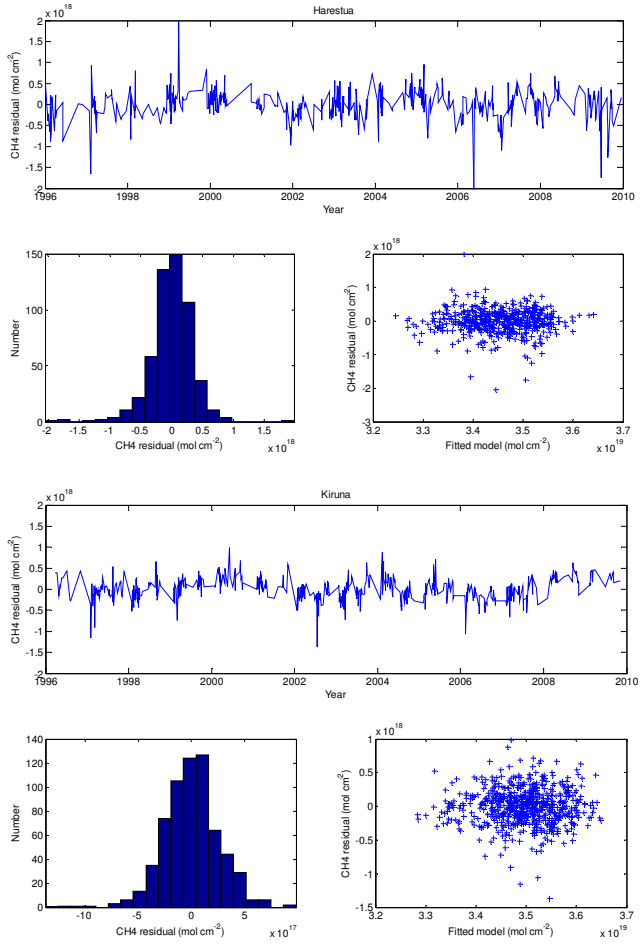

Fig. 6b. CH_4 residuals and distributions of the Harestua and Kiruna FTIR time series.

ACPD
11, 8207–8247, 2011

A new method to detect long term trends of CH_4 and N_2O

J. Angelbratt et al.

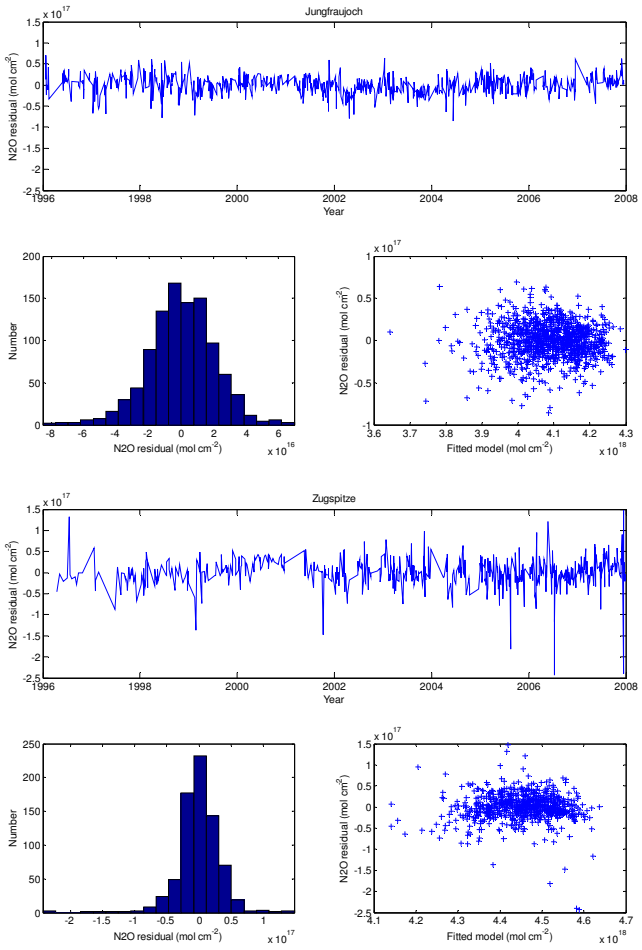

Fig. 7a. N_2O residuals and distributions of the Jungfraujoch and Zugspitze FTIR time series.

ACPD
11, 8207–8247, 2011

A new method to detect long term trends of CH_4 and N_2O

J. Angelbratt et al.

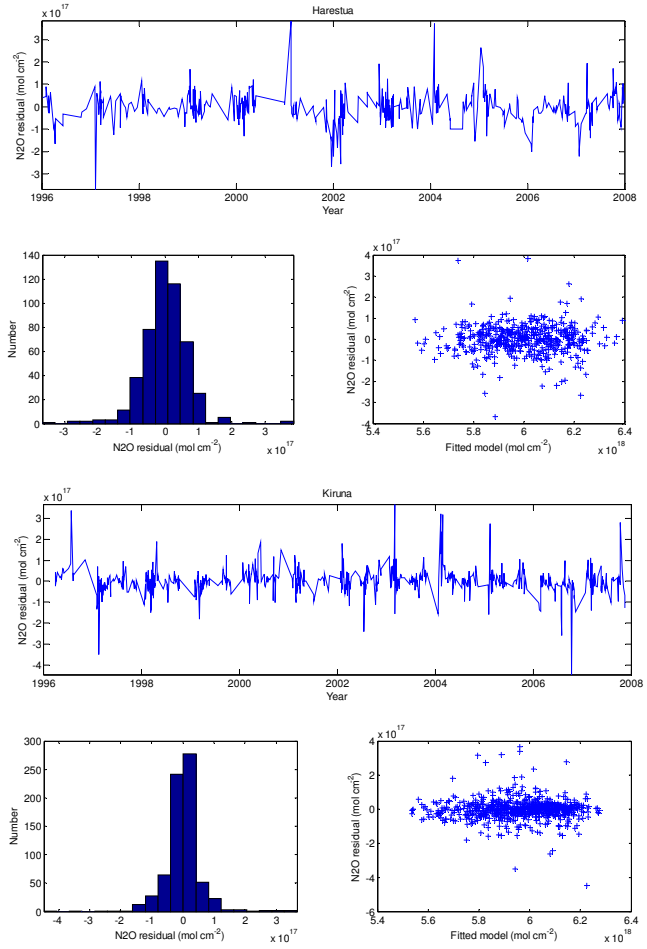

Fig. 7b. N_2O residuals and distributions of the Harestua and Kiruna FTIR time series.

ACPD
11, 8207–8247, 2011